

ORIGINAL RESEARCH PAPER

Pages: 303-315

Dual-Band Printed Dipole Antenna Using Rectangular-Shaped Resonators for 2.4/5.5 GHz WLAN Applications

M. Hosseinnezhad, J. Nourinia, Ch. Ghobadi*Department of Electrical Engineering, Urmia University, Urmia, Iran**mohammadrasoul.hosseinnezhad@gmail.com, j.nourinia@urmia.ac.ir, ch.ghobadi@urmia.ac.ir*Corresponding author: *mohammadrasoul.hosseinnezhad@gmail.com*

DOI: 10.22070/jce.2021.14890.1194

Abstract- A new design of a dual-band printed dipole antenna with integrated balun is presented in this study. The antenna in simple form is composed of a printed dipole, integrated balun, a Γ -shaped feed, and a square-shaped ground plane, which achieves a fundamental resonance at 2.4 GHz frequency. A pair of rectangular-shaped resonators are positioned on two sides of the Γ -shaped feed in the second designing step innovatively to accomplish the additional resonance at 5.5 GHz as the second frequency band of the WLAN. Two electromagnetically coupling mechanisms prepared between the Γ -shaped feed and dipole arms, and rectangular-shaped resonators, which lead to creating two operating frequency bands. An equivalent circuit and a parametric study presented to explain the antenna performance in this work. Experiments approve that the proposed dual-band antenna has two impedance bandwidths of 14.1% (2.23-2.57 GHz) and 25.7% (4.83-6.26 GHz) with average gains of 12.10 dBi and 6.36 dBi over the first and second frequency bands, respectively, which covers the 2.4/5.5 GHz WLAN frequency bands successfully.

Index Terms- Dual-Band Antenna, Printed Dipole, Integrated Balun, WLAN Application.

I. INTRODUCTION

Nowadays, to satisfy the requirements of 802.11a and 802.11b standards for wireless local area network (WLAN) systems to have a high data rate with an excellent reliable communication link, it is necessary to design a compact dual-band antenna. Fundamentally, the WLAN transceivers operate at two distinct frequency bands, i.e., 2.4 GHz (2.4-2.484 GHz) and 5 GHz (5.15-5.825 GHz), which lead to having two individual antennas. This weakness makes some other problems such as increasing the total volume and cost of the system. On the other hand, designing the antennas with impedance bandwidth (IBW) of 2-6 GHz to cover both WLAN frequency bands with stable and same radiation

performance on the operating frequency band is complicated. However, covering the whole frequency band of 2-6 GHz for WLAN makes frequency interference problems with other wireless systems. Nevertheless, designing a compact dual-band antenna that operates at 2.4 GHz and 5.5 GHz frequency bands is beneficial and applicable. In the last few years, numerous dual-band antennas with different designing techniques are reported in the literature [1-12].

Two inverted-F antenna elements are employed to achieve dual-band performance for WLAN application in [1]. In [2], a U-shaped slit was used to generate two frequency bands for WLAN systems with omnidirectional radiation properties. A dual-band WLAN array antenna was investigated in [3]. In this design, two integrated bandpass filters and two rectangular patches were used to excite the WLAN frequency bands in 2.4/5.8 GHz. Besides, in [4], two bowtie-dipole elements with different dimensions are introduced to cover the WLAN frequency bands. In this structure, two integrated baluns with different heights are used to feed the dipoles correspondingly. Furthermore, a compact slot antenna is presented in [5] for 2.4/5.8 GHz WLAN on-body applications composed of an asymmetric T-shaped slot with two long and short paths to achieve dual-band functionality. Other techniques also are employed to generate dual-band capability such as using mushroom-like superstrate structure [6], employing bowtie-radiators [7], etching slots on the patch [8], using metamaterial structures [9], using stacked structures [10], including Complementary Split Ring Resonator (CSRR) [11] and comprising arc-shaped grounded stub [12]. Additionally, Dual-band performance used for other applications such as mobile base-station systems [13] and UHF RFID Tags [14].

Principally, printed dipole antenna with integrated balun is a competent choice for high-gain applications with stabilized radiation pattern, widely used in WLAN systems [15]. Regarding compact size and ease of integration with microwave circuits, the printed antennas are manufactured by using printed circuit board (PCB) technology [16]-[19]. Printed dipole antennas with integrated baluns have inspired the design of firstly reported by Luk in 2006 [20]. Indeed, in this design, the integrated balun acts like a $\lambda/4$ coaxial balun, which converts the unbalanced coaxial line to a balanced slot line to feed the dipole [21] and [22].

A new design of printed dipole antenna with integrated balun is introduced and investigated in this work. It achieved a dual-band functionality by employing rectangular-shaped resonators innovatively. The antenna is composed of an integrated balun with a Γ -shaped feed, a printed dipole, a square-shaped reflector, and a pair of rectangular-shaped resonators placed on two sides of the Γ -shaped feed. According to the equivalent circuit of the antenna, two coupling mechanisms were accomplished. One of them is established between the Γ -shaped feed and the dipole, and the other one is formed between the Γ -shaped feed and the rectangular-shaped resonators.

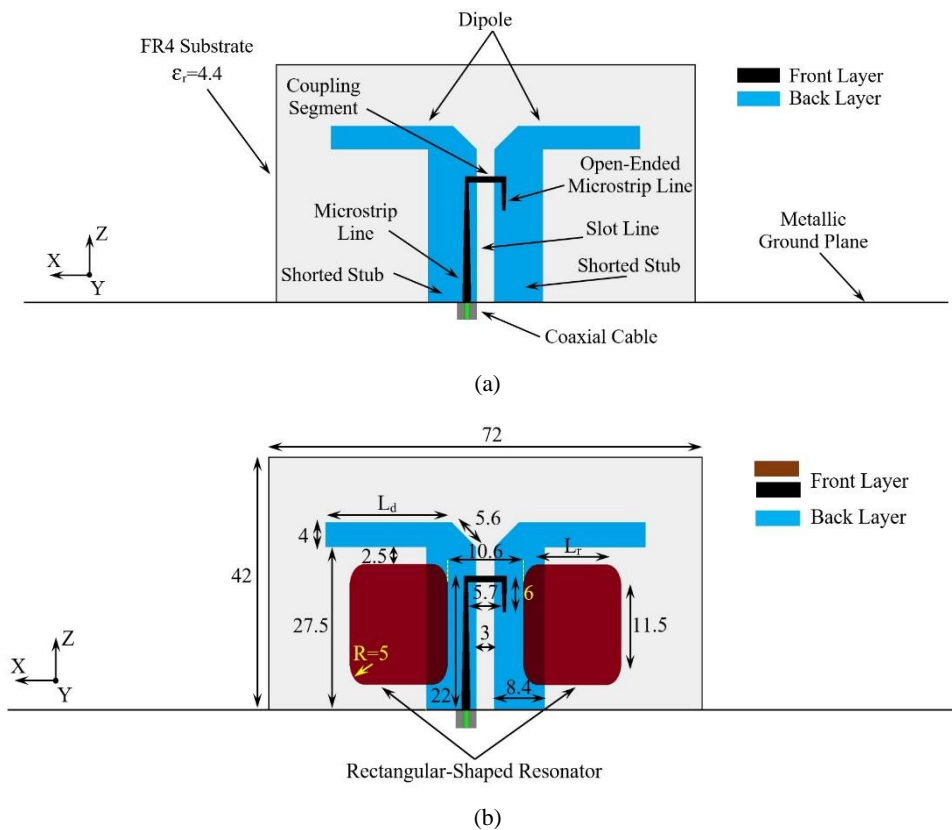


Fig. 1. (a) Geometry of the simple printed dipole antenna with an integrated balun, and (b) Geometry of the proposed dual-band antenna.

II. ANTENNA DESIGN

A simple printed dipole antenna with an integrated balun is proposed at the first step. It is composed of dipole arms and Γ -shaped feed which are printed on the two sides of a $72 \times 42 \text{ mm}^2$ FR4 substrate with 0.8 mm thickness. According to Fig.1 (a), the Γ -shaped feed has three segments, a microstrip line, a coupling segment, and an open-ended microstrip line. In this structure, the input signal delivered to the microstrip line from the coaxial cable, and the coupling segment transfers it to the dipole arms through a slot line. The open-ended microstrip line is in charge of producing excellent impedance matching. It is noteworthy that the dipole is feed by an electromagnetically coupling mechanism like happened in transformers. The length of the dipole arms (L_d) is set at approximately $\lambda_1/4$ in the first frequency resonance of the WLAN operating band, i.e. 2.4 GHz.

At the second step of antenna designing, a pair of rectangular-shaped resonators are located on two sides of the Γ -shaped feed to achieve another resonance at 5.5 GHz as the second frequency band of the WLAN. Indeed additional electromagnetic coupling is accrued between the Γ -shaped feed and rectangular-shaped resonators. Likewise, in this step, the length of the resonators is almost $\lambda_2/4$ for the center frequency of 5.15-5.825 GHz WLAN second operating band. The proposed antenna with dual-

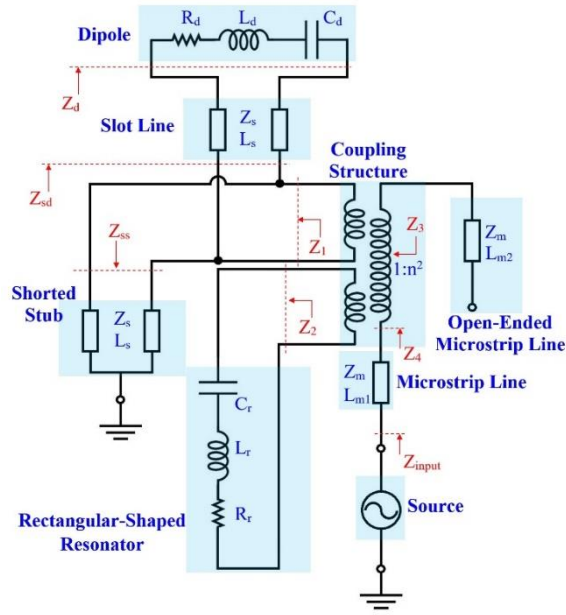


Fig. 2. Equivalent circuit of the proposed dual-band antenna.

band functionality is presented in Fig 1(b). Other dimensions are reported in this figure.

III. EQUIVALENT CIRCUIT OF THE ANTENNA

The proposed dual-band antenna can be modeled as an equivalent circuit, demonstrated in Fig. 2 [23]. The model comprises microstrip lines, RLC circuits, coupling structure, stub, and slot line. Valuable and applicable equations for calculating the properties of a microstrip line given in [24]. By using these formulas, all of the microstrip line characteristics such as the effective permittivity (ϵ_{eff}), wavelength (λ), characteristic impedance (Z_m), and width of the microstrip lines (w) can be calculated. The relative permittivity (ϵ_r) and height of the dielectric substrate (h) assumed to be given.

It is evident in the equivalent circuit of the antenna that the input signal is delivered to a coupling structure through a microstrip line with the characteristic impedance of Z_m and length of L_{m1} . An ideal transformer with two secondary windings associated with two coupling mechanisms with a ratio of $1:n^2$ exhibits the coupling structure. Furthermore, an open-ended microstrip line that compensates for the impedance matching represents the last portion of the Γ -shaped feed. The couplings were performed between the Γ -shaped feed and printed dipole and also rectangular-shaped resonators. The printed dipole and rectangular-resonator are modeled as RLC circuits with the input impedance of Z_d and Z_2 , respectively. By using of equations presented in [25], the input impedance of the printed dipole with the length of $2 \times L_d$ can be calculated as follows

$$Z_d = \frac{120 \left(\ln \frac{16L_d}{w} - 1 \right)}{\cosh(4\alpha L_d) - \cos(4\beta L_d)} \left(\left(\sinh(4\alpha L_d) - \frac{\alpha}{\beta} \sin(4\beta L_d) \right) - j \left(\frac{\alpha}{\beta} \sinh(4\alpha L_d) + \sin(4\beta L_d) \right) \right) \quad (1)$$

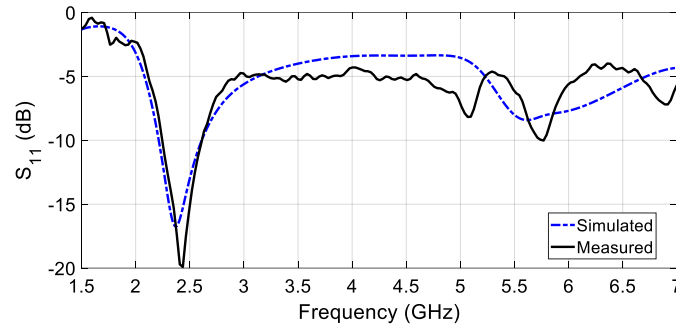


Fig. 3. Simulated and measured S_{11} of the proposed antenna in simple form.

In this equation, α and β represent the attenuation coefficient and the phased shift coefficient of the surface current on the printed dipole, respectively, and w is the width of dipole arms. A similar equation can be defined for the rectangular-shaped resonators, which is introduced by Z_2 . The addressed impedances in the equivalent circuit of the antenna such as Z_1 , Z_3 , Z_4 , Z_{sd} , and Z_{input} can be calculated using the transmission line theories as follows [26]

$$Z_1 = Z_{sd} \parallel Z_{ss} \quad (2)$$

$$Z_3 = n^2(Z_1 \parallel Z_2) \quad (3)$$

$$Z_4 = Z_3 - jZ_m \cot \beta L_{m2} \quad (4)$$

$$Z_{sd} = Z_s \frac{Z_d + jZ_s \tan(\beta L_s)}{Z_s + jZ_d \tan(\beta L_s)} \quad (5)$$

$$Z_{input} = Z_m \frac{Z_4 + jZ_m \tan \beta L_{m1}}{Z_m + jZ_4 \tan \beta L_{m1}} \quad (6)$$

The delivered signal to the Γ -shaped feed transferred to the printed dipole and rectangular-shaped resonators electromagnetically. It leads to generating two impedance bandwidths for dual-band WLAN applications.

IV. SIMULATION AND EXPERIMENTAL RESULTS

All of the simulation and experimental results carried out using HFSS Ver.15 software and an Agilent E8363C Network Analyzer, respectively. The simulated and measured S_{11} results of the simple printed dipole antenna with an integrated balun are shown in Fig 3. According to the experiments, the antenna in simple form has an impedance bandwidth of 15.3% (2.23-2.60 GHz), which covers the 2.4 GHz WLAN frequency band. The length of dipole arms has a fundamental role in determining the location of the main resonance frequency. A parametric study is depicted in Fig. 4, which shows the resonance frequency of the antenna shifts from 2.65 GHz to 2.32 GHz by increasing

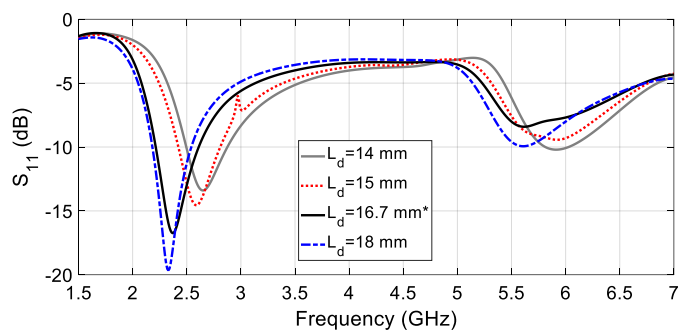


Fig. 4. Simulated S_{11} response of the proposed antenna in simple form for various lengths of L_d .

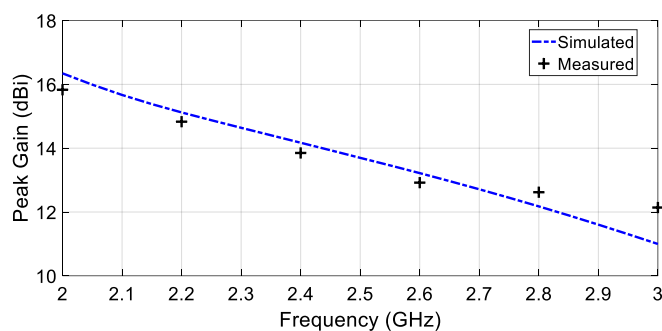


Fig. 5. Simulated and measured peak gains of the simple printed dipole antenna.

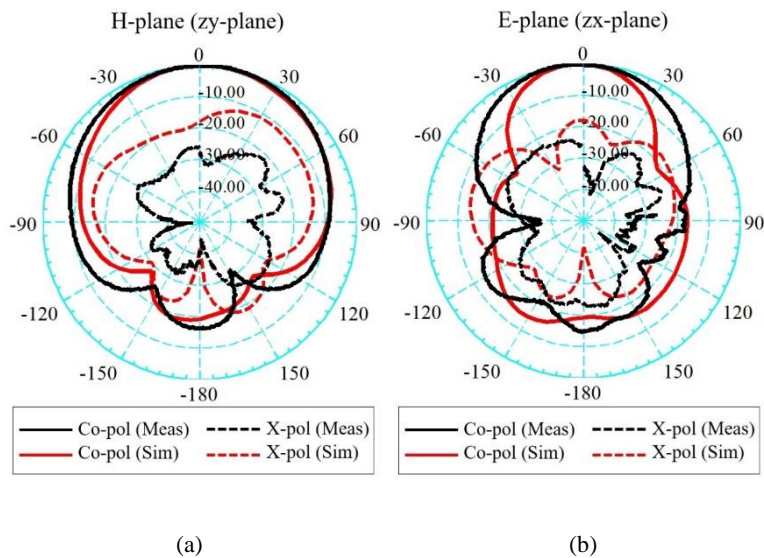


Fig. 6. Simulated and measured (a) H-plane and (b) E-plane radiation patterns of the simple printed dipole antenna at 2.4 GHz frequency.

the L_d from 14 mm to 18 mm.

In this design, the L_d is set at 16.7 mm to achieve resonance at 2.39 GHz. Furthermore, the simulated and measured peak gains of the simple printed dipole antenna are plotted in Fig. 5.

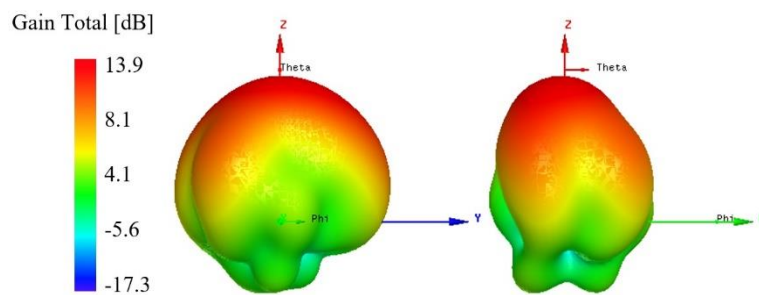


Fig. 7. Simulate 3D-radiation patterns of the simple printed dipole antenna at 2.4 GHz frequency.

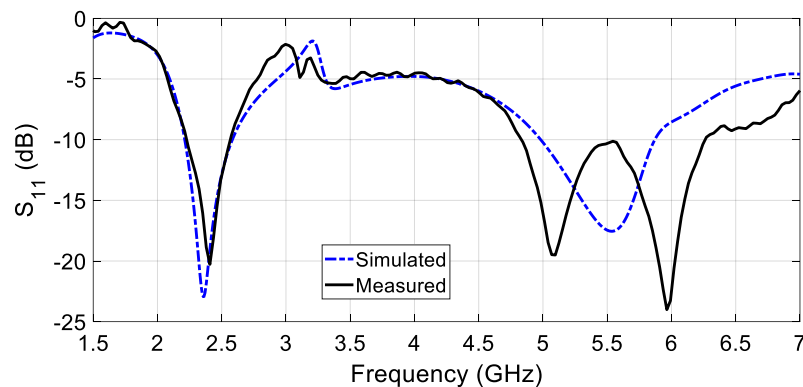


Fig. 8. Simulated and measured S_{11} of the proposed dual-band antenna.

Numerical results confirm that the antenna has an average gain of 13.70 dBi over the operating frequency band.

2D normalized and 3D radiation patterns in yz - and xz -planes at 2.4 GHz are presented in Fig. 6 and Fig. 7. Results show that the radiation patterns of the antenna are stable and unidirectional. The cross-polarization and the back-lobe of the antenna radiation patterns are relatively weak. Moreover, the rectangular-shaped resonators are placed on two sides of the Γ -shaped feed to realize an additional operating band at 5.5 GHz. The numerical and experimental S_{11} curves of the proposed dual-band antenna are reported in Fig. 8. Regarding the results, the proposed dual-band antenna has impedance bandwidths of 14.1% (2.23-2.57 GHz) and 25.7% (4.83-6.26 GHz), which is cover the 2.4/5.5 GHz WLAN frequency bands successfully. The simulated and measured peak gains of the proposed dual-band antenna illustrated in Fig. 9 over the frequency bands. The proposed antenna has average gains of 12.10 dBi and 6.36 dBi over the first and second frequency bands.

The normalized H-plane radiation patterns of the proposed dual-band antenna are demonstrated in Fig. 10 at frequencies of 2.4 GHz and 5.5 GHz. It is shown that the proposed antenna has HPBW of about 82.6° , and 123° at frequencies of 2.4 GHz, and 5.5 GHz, respectively.

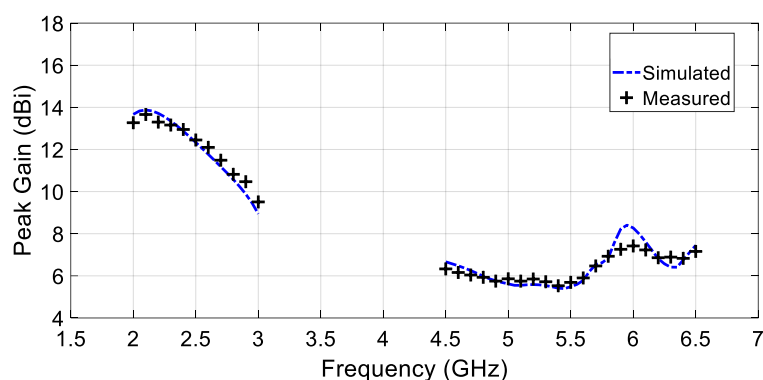


Fig. 9. Simulated and measured peak gains of the proposed dual-band antenna.

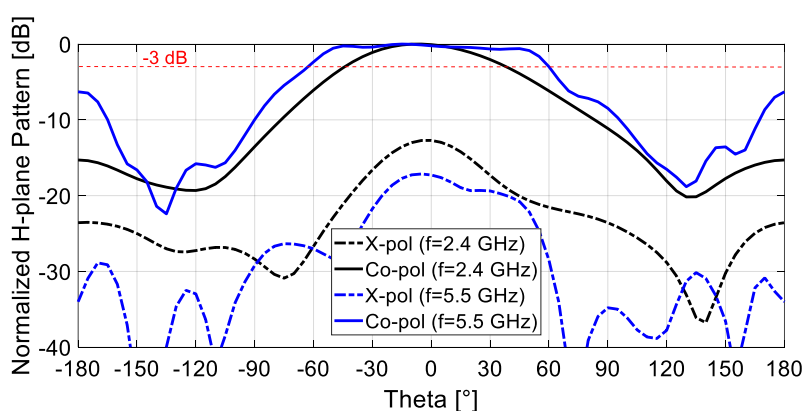


Fig. 10. Simulated normalized H-plane radiation patterns of the proposed dual-band antenna.

Moreover, the cross-polarizations at least 12 dB are lower than the co-polarizations. 2D normalized and 3D radiation patterns of the proposed antenna in yz - and xz -planes at 2.4 GHz and 5.5 GHz are presented in Fig. 11 and Fig. 12, correspondingly. The proposed antenna has stable and unidirectional radiation patterns. Theoretical and experimental results of the presented design have a slight discrepancy that can be caused by human errors and fabrication tolerances. Photographs of the measurement setup are shown in Fig. 13.

Furthermore, the current distribution over the proposed antenna at the resonant frequencies (i.e. 2.4 GHz and 5.5 GHz) is shown in Fig. 14. The concentration of current flow over the dipole arms and parasitic element, which is shown in this figure, determines the antenna's dual-band performance at 2.4 and 5.5 GHz.

Also Table 1 displays a comparison between the proposed antenna in this work and similar dual-band antennas in terms of impedance bandwidth, HPBW, average gain, and dimensions. It is seen that compared to other dual-band antennas, the proposed antenna has a higher gain and lower dimensions.

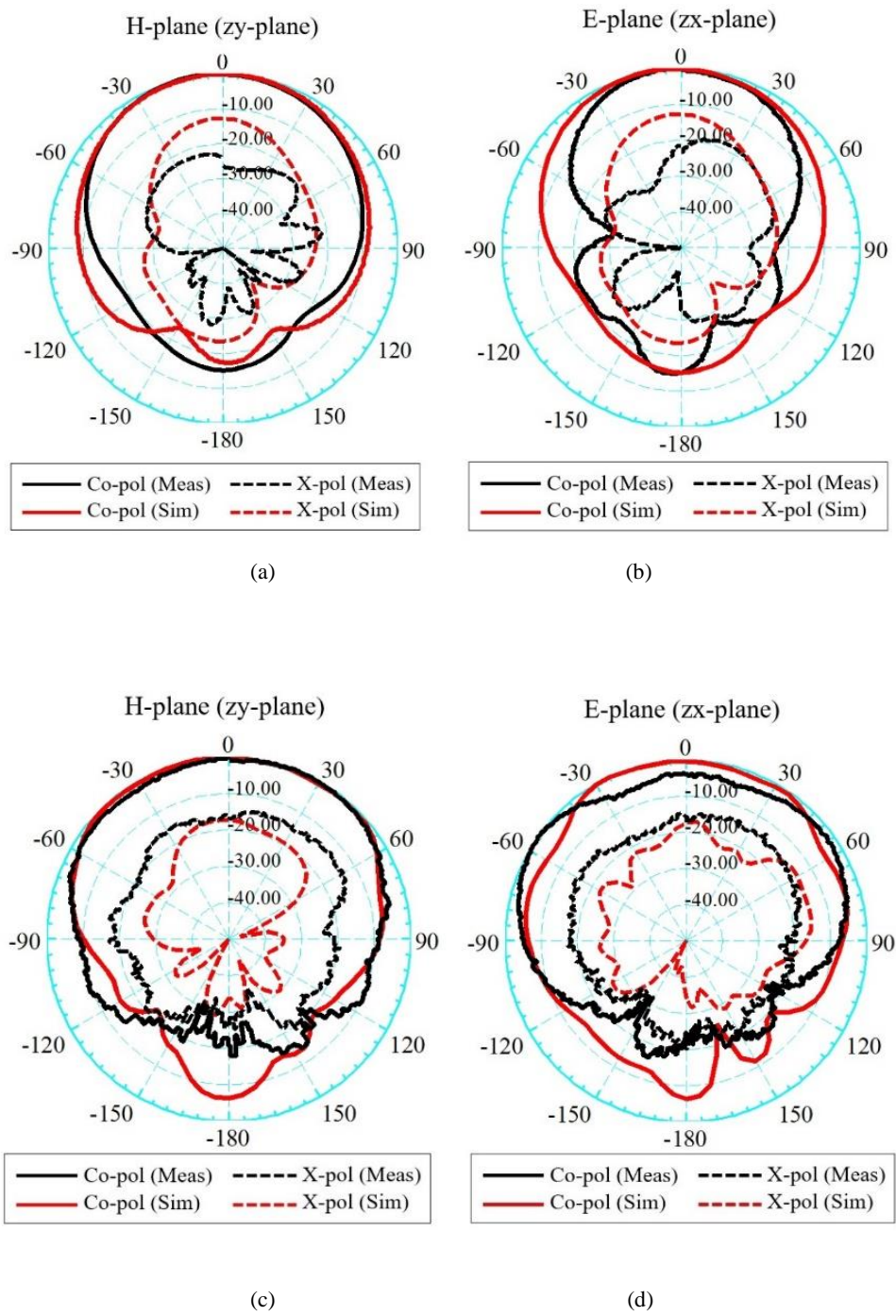


Fig. 11. Simulated and measured (a) and (c) H-plane, and (b) and (d) E-plane radiation patterns of the proposed dual-band antenna at (a) and (b) 2.4 GHz and (c) and (d) 5.5 GHz frequency.

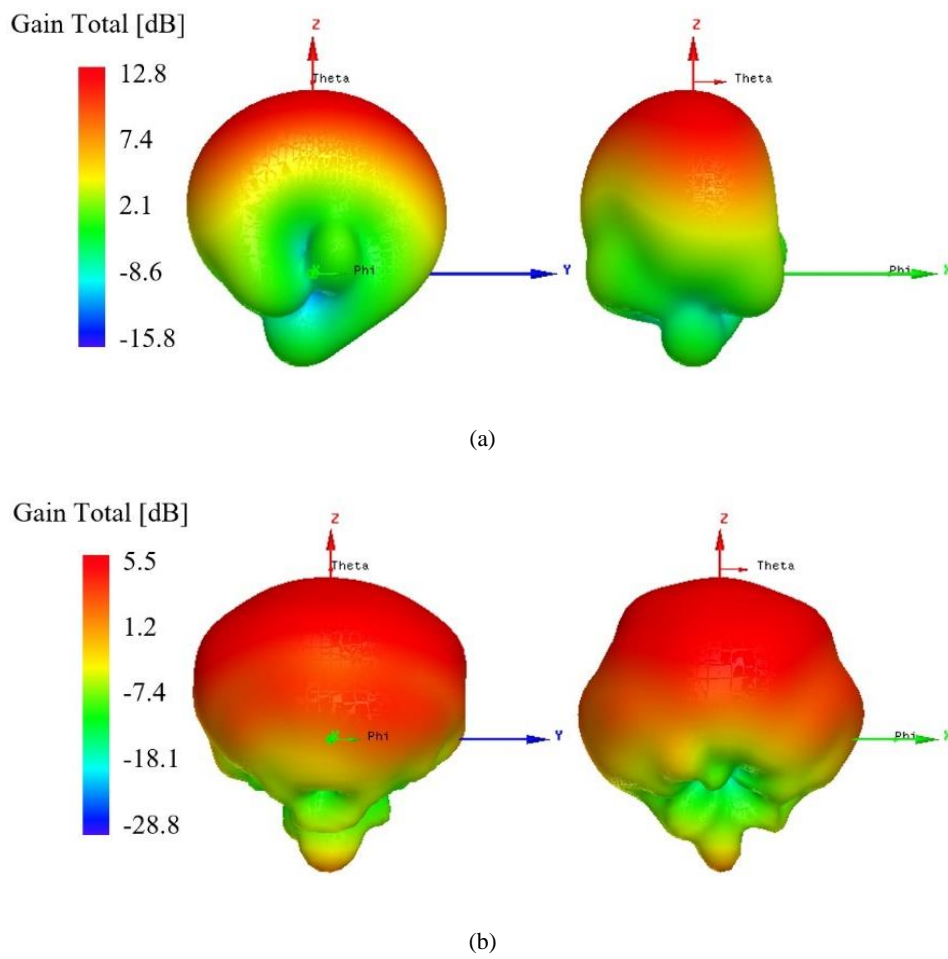


Fig. 12. Simulate 3D-radiation patterns of the proposed dual-band antenna at (a) 2.4 GHz and (b) 5.5 GHz frequency.

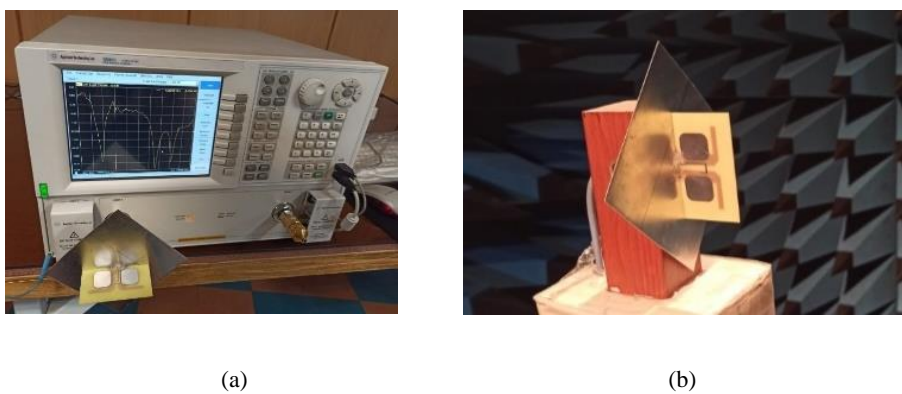
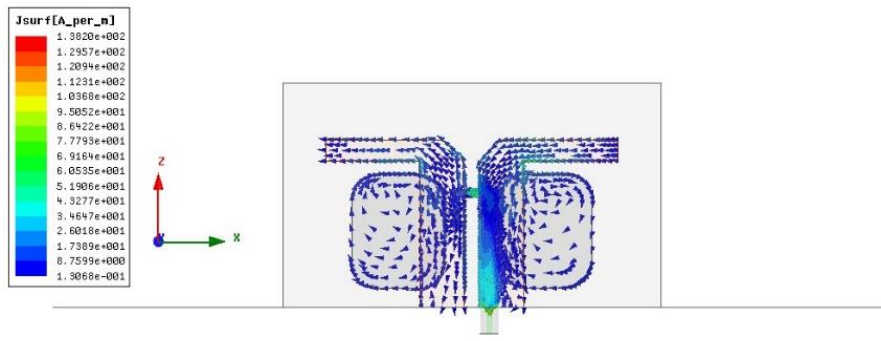
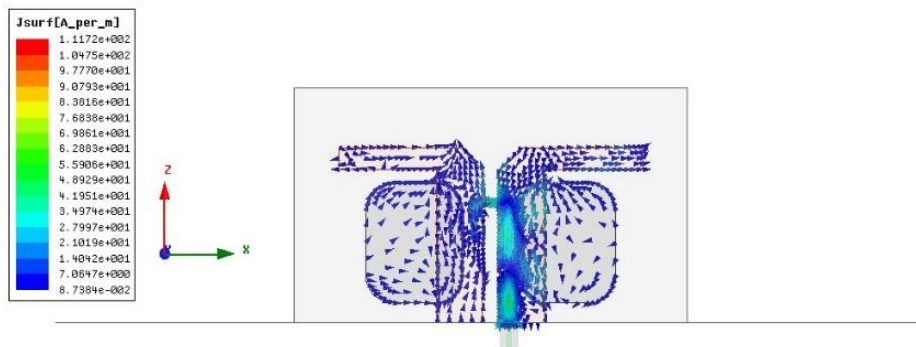


Fig. 13. Photographs of the (a) S_{11} measurement setup using VNA, and (b) antenna connected to the Spectrum Analyzer in the anechoic chamber.



(a)



(b)

Fig. 14. Current distribution over the proposed antenna at the resonant frequencies (a) 2.45 GHz, and (b) 5.5 GHz

Table 1 Size and performance comparison of dual-band antennas.

Refs.	Impedance BW (GHz)/FBW (%)	HPBW (deg)	Ave. Gain (dBi)	Dimensions (λ_0^3)
[1]	2.37–2.53/ 6.5 4.79–5.93/ 5.5	NR	NR	1.13×0.76×0.02
[2]	2.34–2.5 / 6 5.06–5.91/ 15	NR	4 6	1.05×0.38×0.24
[4]	2.36–2.76/ 15.6 5.12–5.62/ 9.3	NR	7 7.1	1.4×1.44×0.09
[13]	0.80–0.92/13.4 1.71–2.08/19.8	105.4 83.3	9.2 7.8	1.03×1.03× 0.21
This work	2.23–2.57 / 14.1 4.83–6.26 / 25.7	82.6 123	12.10 6.36	1.02×0.6×0.01

FBW: Fractional Bandwidth, NR: Not Reported.

V. CONCLUSION

A printed dipole antenna with an integrated balun and rectangular-shaped resonator introduced and investigated in this paper, which attains a dual-band functionality by employing two electromagnetically coupling mechanisms in novatively. The proposed dual-band dipole antenna printed on a 72×42 mm² FR4-substrate covering the 2.4/5.5 GHz WLAN frequency bands with average gains of 12.10 dBi and 6.36 dBi.

ACKNOWLEDGMENT

The authors would like to express their special gratitude to the Northwest Antenna and Microwave Research Laboratory (NAMRL) at Urmia University for fabrication and testing the antenna.

REFERENCES

- [1] J. Deng, J. Li, L. Zhao, and L. Guo, "A Dual-Band Inverted-F MIMO Antenna with Enhanced Isolation for WLAN Applications," *IEEE Antennas and Wireless Propagation Letters*, vol. 16, pp. 2270–2273, June 2017.
- [2] Q. Gong, M. Xiao, P. Luo, and Y. Cui, "Dual-band horizontally/dual-polarized antennas for WiFi/WLAN/ISM applications," *Microwave and Optical Technology Letters*, vol. 62, no. 3, pp. 1398–1408, Nov. 2019.
- [3] W. Ahmad and D. Budimir, "Dual-band WLAN antenna array with integrated bandpass filters for harmonic suppression," *2015 IEEE International Symposium on Antennas and Propagation & USNC/URSI National Radio Science Meeting*, July 2015.
- [4] H. Zhai, K. Zhang, S. Yang, and D. Feng, "A Low-Profile Dual-Band Dual-Polarized Antenna with an AMC Surface for WLAN Applications," *IEEE Antennas and Wireless Propagation Letters*, vol. 16, pp. 2692–2695, Aug. 2017.
- [5] K.-L. Wong, H.-J. Chang, C.-Y. Wang, and S.-Y. Wang, "Very-Low-Profile Grounded Coplanar Waveguide-Fed Dual-Band WLAN Slot Antenna for On-Body Antenna Application," *IEEE Antennas and Wireless Propagation Letters*, vol. 19, no. 1, pp. 213–217, Jan. 2020.
- [6] Z. Wu, L. Li, X. Chen, and K. Li, "Dual-Band Antenna Integrating With Rectangular Mushroom-Like Superstrate for WLAN Applications," *IEEE Antennas and Wireless Propagation Letters*, vol. 15, pp. 1269–1272, Dec. 2015.
- [7] A. Dadgarpour, B. Zarghooni, T. A. Denidni, and A. A. Kishk, "Dual-Band Radiation Tilting Endfire Antenna for WLAN Applications," *IEEE Antennas and Wireless Propagation Letters*, vol. 15, pp. 1466–1469, Dec. 2015.
- [8] W.-C. Liu, C.-M. Wu, and N.-C. Chu, "A compact low-profile dual-band antenna for WLAN and WAVE applications," *AEU - International Journal of Electronics and Communications*, vol. 66, no. 6, pp. 467–471, June 2012.
- [9] M. Tamrakar and U. K. Kommuri, "Dual Band CRLH Metal Antenna for WLAN Applications," *Wireless Personal Communications*, vol. 116, no. 4, pp. 3235–3246, Sept. 2020.
- [10] J.-S. Row and Y.-J. Huang, "Dual-band dual-polarized antenna for WLAN applications," *Microwave and Optical Technology Letters*, vol. 60, no. 1, pp. 260–265, Dec. 2017.
- [11] H. Yao, X. Liu, H. Zhu, H. Li, G. Dong, and K. Bi, "Dual-Band Microstrip Antenna Based on Polarization Conversion Metasurface Structure," *Frontiers in Physics*, vol. 8, Sept. 2020.
- [12] R.-H. Li, X.-W. Shi, N. Zhang, Y.-F. Wang, and Y.-J. Wang, "A novel compact dual-band antenna for WLAN applications," *Microwave and Optical Technology Letters*, vol. 54, no. 6, pp. 1476–1479, June 2012.

- [13] S. Khorasani, J. Nourinia, C. Ghobadi, M. Shokri, A. Hatamian, and B. Virdee, "Dual-band magneto-electric dipole antenna with high-gain for base-station applications," *AEU - International Journal of Electronics and Communications*, vol. 134, p. 153696, March 2021.
- [14] H. Bouazza, A. Lazaro, M. Bouya, and A. Hadjoudja, "A Planar Dual-Band UHF RFID Tag for Metallic Items," *Radioengineering*, vol. 29, no. 3, pp. 504–511, Sept. 2020.
- [15] R. Nasirzade, J. Nourinia, C. Ghobadi, M. Shokri, and R. Naderali, "Broadband printed MIMO dipole antenna for 2.4 GHz WLAN applications," *Journal of Instrumentation*, vol. 15, no. 01, Jan. 2020.
- [16] A. Siahcheshm, J. Nourinia, C. Ghobadi, and M. Shokri, "Circularly Polarized Printed Helix Antenna for L- and S-Bands Applications," *Radio engineering*, vol. 29, no. 1, pp. 67–73, April 2020.
- [17] A. Eslami, J. Nourinia, C. Ghobadi, and M. Shokri, "Four-element MIMO antenna for X-band applications," *International Journal of Microwave and Wireless Technologies*, pp. 1–8, Jan. 2021.
- [18] Z. Amiri, S. Movagharnia, M. Masoumi, M. Shokry, and B. S. Virdee, "Extremely wideband printed monopole antenna with dual rejection bands," *Microwave and Optical Technology Letters*, vol. 58, no. 4, pp. 908–911, Feb. 2016.
- [19] S. Mirzaee and Y. Zehforoosh, "CPW-Fed Circularly Polarized Slot Antenna with Elliptical-Shaped Patch for UWB Applications," *Journal of Communication Engineering*, vol. 6, no. 2, pp. 151–162, Dec. 2017.
- [20] K. M. Luk and H. Wong, "A new wideband unidirectional antenna element," *Int. J. Microw. Opt. Technol.*, vol. 1, no. 1, pp. 35–44, Jan. 2006.
- [21] R. L. Li, T. Wu, B. Pan, K. Lim, J. Laskar, and M. Tentzeris, "Equivalent-Circuit Analysis of a Broadband Printed Dipole With Adjusted Integrated Balun and an Array for Base Station Applications," *IEEE Trans. Antennas and Propag.*, vol. 57, no. 7, pp. 2180–2184, July 2009.
- [22] Y. Gou, S. Yang, J. Li, and Z. Nie, "A Compact Dual-Polarized Printed Dipole Antenna With High Isolation for Wideband Base Station Applications," *IEEE Trans. Antennas and Propag.*, vol. 62, no. 8, pp. 4392–4395, Aug. 2014.
- [23] W. Choe and J. Jeong, "A Broadband THz On-Chip Transition Using a Dipole Antenna with Integrated Balun," *Electronics*, vol. 7, no. 10, p. 236, Oct. 2018.
- [24] M. B. Steer, *Microwave and RF design a systems approach*. Edison, NJ: Scitech Publishing, 2015.
- [25] I. Rana and N. Alexopoulos, "Current distribution and input impedance of printed dipoles," *IEEE Tran. Antennas and Propag.*, vol. 29, no. 1, pp. 99–105, Jan. 1981.
- [26] D. M. Pozar, *Microwave engineering*. New Delhi: Wiley India, 2017.